SPECIAL TOPIC — Physical research in liquid crystal

High signal-to-noise ratio sensing with Shack–Hartmann wavefront sensor based on auto gain control of electron multiplying CCD*

Zhao-Yi Zhu(朱召义)[1,2], Da-Yu Li(李大禹)[1], Li-Fa Hu(胡立发)[1], Quan-Quan Mu(穆全全)[1], Cheng-Liang Yang(杨程亮)[1], Zhao-Liang Cao(曹召良)[1], and Li Xuan(宣丽)[1,†]

[1] *State Key Laboratory of Applied Optics, Changchun Institute of Optics, Fine Mechanics and Physics, Chinese Academy of Sciences, Changchun* 130033, *China*

[2] *University of Chinese Academy of Sciences, Beijing* 100049, *China*

(Received 25 May 2016; published online 20 July 2016)

High signal-to-noise ratio can be achieved with the electron multiplying charge-coupled-device (EMCCD) applied in the Shack–Hartmann wavefront sensor (S–H WFS) in adaptive optics (AO). However, when the brightness of the target changes in a large scale, the fixed electron multiplying (EM) gain will not be suited to the sensing limitation. Therefore an auto-gain-control method based on the brightness of light-spots array in S–H WFS is proposed in this paper. The control value is the average of the maximum signals of every light spot in an array, which has been demonstrated to be kept stable even under the influence of some noise and turbulence, and sensitive enough to the change of target brightness. A goal value is needed in the control process and it is predetermined based on the characters of EMCCD. Simulations and experiments have demonstrated that this auto-gain-control method is valid and robust, the sensing SNR reaches the maximum for the corresponding signal level, and especially is greatly improved for those dim targets from 6 to 4 magnitude in the visual band.

Keywords: adaptive optics, Shack–Hartmann wavefront sensor, electron multiplying charge-coupled-device (EMCCD), auto-gain-control method

PACS: 07.07.Df, 95.75.Qr, 95.55.Cs **DOI:** 10.1088/1674-1056/25/9/090702

1. Introduction

Adaptive optics (AO) has been widely used in various research areas,[1–3] such as astronomical observation by ground-based telescopes. In AO systems, the Shack–Hartmann wavefront sensor (S–H WFS) has been most popularly used for its high speed and high precision.[4–6] It consists of a lenslet array followed by a CCD detector. The incoming light is sampled by the lenslet array at the front, and then focused onto the CCD detector which outputs an image of light-spots array. The light-spot centroids of the array are used to calculate the slopes of the corresponding sub-wavefronts, and the total disturbed wavefront can be retrieved by all of the sub-wavefronts.[7–9]

The astronomical objects are usually very dim, which brings challenges to the AO systems, especially to wavefront sensing. The S–H WFS is designed using a sub-aperture method that the local light spots in the array are formed by the light collected in sub-apertures. The collected light is proportional to the sub-aperture size which is typically equal to the atmospheric coherent length r_0. For example, when observing a star of 6 magnitude in visual band (6^{mv}) by an S–H WFS designed at $r_0 = 10$ cm, the photon number collected in a sub-aperture is almost 100. Suppose that the light spot is recorded by an ordinary CCD with 4 pixels, if the readout noise of the CCD is 25 e^-/pixel/frame, the light spot will be lost in the noise and the sensing will fail.

A new kind of CCD detector called an electron multiplying charge-coupled-device (EMCCD)[10–12] has achieved sub-electron readout noise through the electron multiplication technique which makes wavefront sensing very efficient.[13–15] Of course, S–H WFS with the EMCCD has higher sensitivity than an ordinary CCD. However, EMCCD's potential sometimes may be lost as the electron multiplying (EM) gain does not match the brightness of an observed object. For example, satellites circle the earth so fast that their brightness will change in a large range within a few minutes. In this case, a fixed EM gain is not suitable for sensing, and auto-gain-control based on the real-time brightness of the target is necessary.

The conventional gain control methods such as those based on the gray level histogram[16] or setting thresholds[17] are proposed for the normal image systems, but are not applicable for S–H WFS. For S–H WFS, most light of the target is focused into these light spots of the output array, and large parts of CCD pixels are with few signals. Furthermore, the signal distributions of each light spot are different from each other and change from frame to frame due to the turbu-

*Project supported by the National Natural Science Foundation of China (Grant Nos. 11174274, 61205021, and 61405194) and the State Key Laboratory of Applied Optics, Changchun Institute of Optics, Fine Mechanics and Physics, Chinese Academy of Sciences.

†Corresponding author. E-mail: xuanli@ciomp.ac.cn

© 2016 Chinese Physical Society and IOP Publishing Ltd

lence and the scintillation, and the statistics of the pixel signals are totally different between frames. Another thing is that the histogram- or thresholds-based methods compare all the pixels, do ordering and counting among all pixels, which is a huge treatment burden and is not suitable for the real-time working AOS. The third is that when the brightness of the observed targets changes fiercely, a high EM gain will easily cause the self-protection of the EMCCD which must be avoided during the sensing in AOSs.

In this paper, we first analyze the characters of the light-spots array. Then an average value based on the light-spots array is proposed to be the control value for the auto-gain-control method, and the characters of the proposed control value are analyzed. The control value and the control method are verified in the experiments, and the signal-to-noise ratio (SNR) is applied to analyze the improvement brought by the auto-gain-control method.

2. Principle of the auto-gain-control

2.1. Analysis of light-spots array

Due to the atmospheric turbulence, the wavefront of the incoming light is disturbed, resulting in light spots dislocated from the reference centers and uneven brightness for each light spot in the array. A typical image of light-spots array output by S–H WFS is shown in Fig. 1.

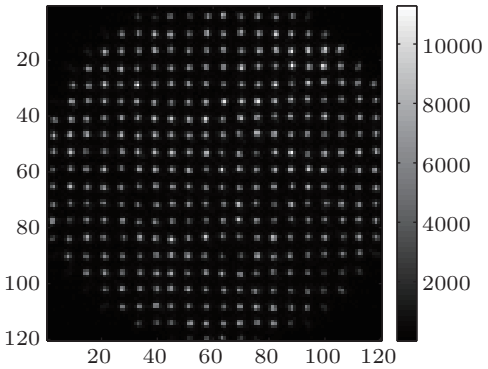


Fig. 1. Typical image of light-spots array output by S–H WFS.

Figure 2 records the maximum signal in the same sub-aperture for 500 continuous frames. The signal ranges from 2000 ADU to 7500 ADU and changes randomly according to time. Due to rapid changing and big differences, it is difficult for the reference methods to characterize the current brightness of the target through the light-spots array. The other problem is that sometimes the telescope may miss following the targets due to this rapid movement. Under this circumstance only parts of lenslets are illuminated, the light-spots images lost some spots compared with normal situations. As shown in Fig. 3, pixel numbers counted as control values by the threshold method and the histogram method will change, the predetermined control values become invalid, which leads to a wrong gain.

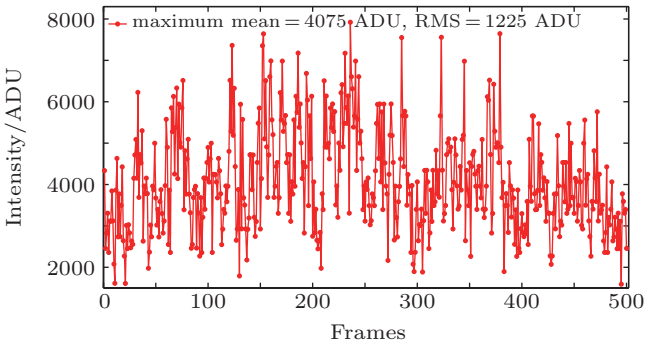


Fig. 2. (color online) The maximum signal in a sub-aperture in 500 continuous frames.

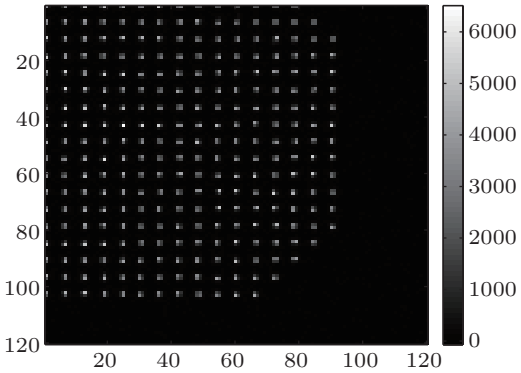


Fig. 3. Output light-spots array of S–H WFS in the missing following case.

2.2. Gain control value design

From the typical output spots image of Fig. 1 or Fig. 3, the disordered light-spots array embodies the most features of S–H WFS. Hence we propose a new method to compute the control value based on the light-spots array: pick up the maximum signal of each light-spot, then calculate the average of the chosen maximum signals, and the average value is adopted as the control value,

$$V_{\text{con}} = \text{mean}(\max_1 \{I_{n\times n}\}, \max_2 \{I_{n\times n}\}, \ldots, \max_k \{I_{n\times n}\}), \quad (1)$$

with $I_{n\times n}$ being the intensity of the $n \times n$ pixels in a sub-window, $\max\{\cdot\}$ picking the maximums, $\text{mean}(\cdot)$ computing the average value, and k the number of the sub-apertures illuminated.

With the exposure function defined, the brightness of the CCD pixel satisfies a linear relationship between the intensity of incident light and the electron multiplication gain expressed as $B = k \times I \times G$.[18] In S–H WFS, the control value we proposed should fulfill this status which will be proved in the following simulations and experiments. In the sensing process, a sufficiently high SNR is needed to overcome the readout noise of the CCD detector by setting a relatively high gain, but high gain may cause the CCD self-protection which should be

avoided. Therefore a goal control is determined by the linearity of the control value and the self-protection process.

Both the control value and the goal control value follow the exposure function, and the relations will be

$$V_{\text{con}} = kI_{\text{target}}G, \tag{2}$$

$$V_{\text{goal}} = kI_{\text{target}}G_{\text{goal}}, \tag{3}$$

$$G_{\text{goal}} = \frac{V_{\text{goal}}}{V_{\text{con}}}G. \tag{4}$$

In the EMCCD system, the control value is calculated from the output image and the gain is set to multiply the next frame image learnt from the EMCCD structure, as shown in the block diagram of the designed controller in Fig. 4. Therefore, the EM gain will be calculated by

$$G_{\text{next}} = \frac{V_{\text{goal}}}{V_{\text{current}}}G_{\text{current}}. \tag{5}$$

Once the EMCCD self-protection process is triggered, it will reset the EM gain to 1, which will break off the observation and must be avoided during the AO process. Here in this paper, an OCam2 EMCCD produced by e2v technologies is applied in the S–H WFS, and a strict limit is adopted. When more than 100 pixels with signal larger than half of the full-well signal exist in the same frame and that lasts for 3 frames, the self-protection will work. The EM register of the OCam2 EMCCD is 14 bit, and the half full-well signal is $2^{14}/2 = 8192$ ADU. This condition should be considered in determining the goal control value.

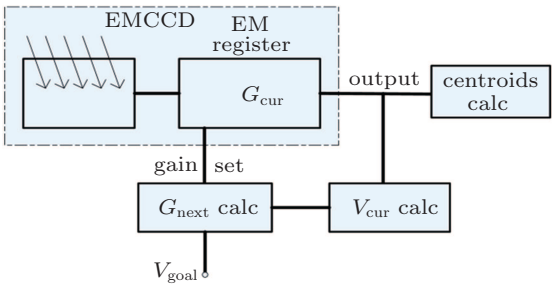


Fig. 4. (color online) The block diagram of the controller combined with the EMCCD.

3. Simulations

3.1. S–H WFS simulation

A simulation based on the S–H WFS is illustrated in this section.[5] Table 1 is the parameters of the S–H WFS. Atmospheric affection simulations are based on an optical device called a turbulence simulator.[21] The phase plate data of the turbulence simulator is used to simulate the turbulent wavefront. Different photon numbers collected in the sub-apertures are applied to simulate the scintillation, the photon numbers in the paper are the average numbers of the sub-apertures in a frame, which is calculated based on the magnitude of the observed target. The normalized intensity distribution function of the light spot is calculated from the sampled sub-wave fronts by the discrete Fourier transform. Signals of pixels in a light spot are obtained by multiplying the normalized intensity distribution function with the photons number in the sub-aperture. The photon spot noise which submits the Poisson distribution is added. An auto-controlled EM gain is then multiplied. A second time of Poisson function affects the multiplied signal to simulate the noises generated by the multiplying influence.[20] A Gaussian readout noise with zero mean and a variance of $\sigma_{\text{r}}^2 = 36$ ADU^2 is also mixed into the pixel signals.

Table 1. Parameters of the S–H WFS components, lenslet array, and CCD220*. Airy spot size follows the formula $D_{\text{airy}} = 2 \times 1.22 \times D_{\text{len}} \times \lambda/f$ with $\lambda = 0.55$ μm.

Parameters	Value
Lenslet array	20×20 (square)
Lenslet diameter	288 μm
Lenslet focal length	19.35 mm (calibrated)
CCD pixels	120×120
CCD pixel size	48 μm
Pixels for each lenslet	288 μm/48 μm = 6 × 6
Airy spot size	90 μm
Pixels for an airy spot	90 μm/48 μm = 1.88×1.88
Readout noise	6 ADU/pixel

*CCD220 developed by e2v technologies (UK) 2 × 2 binning in use.

3.2. Characters of the control value

Based on the simulations, we had got frames of spot image, and the proposed average control value and the maximum value of each frame were calculated respectively. From Fig. 5 we could conclude that the average control value of S–H WFS is in a linear relation with the incident light (see Fig. 5(a)) and the set EM gain (see Fig. 5(b)). The maximum signals, the root-mean-square (RMS) of the control value, and the RMS of the maximum signals were in a similar linear relationship. Based on the measurement data, the function coefficients could be calculated. Therefore we rewrite the exposure function as

$$B = kN_{\text{aper}}G, \tag{6}$$

where N_{aper} is the average photon number collected in a sub-aperture, G is for the EM gain, different k are calculated from different B lines, which indicates the control value, the maximum value, the RMS of control value, and the RMS of the maximum value, respectively. Results were listed in Table 2.

Table 2. Values of different k.

k	k_{con}	k_{max}	$k_{\text{RMS,con}}$	$k_{\text{RMS,max}}$
value	0.0145	0.0295	1.80×10^{-4}	0.0022

Moreover, the control values were compared in different strengths of turbulence. The S–H WFS in our experiments

consisted of a 10-cm-diameter circle sub-aperture at the aperture of the telescope. Different r_0 indicated different strengths of turbulence as 10 cm, 9 cm, 8 cm, and 7 cm, respectively. Figure 6 compared the control values under different intensities of turbulence. With different photons collected in the same sub-aperture, the control values under different r_0 were almost the same.

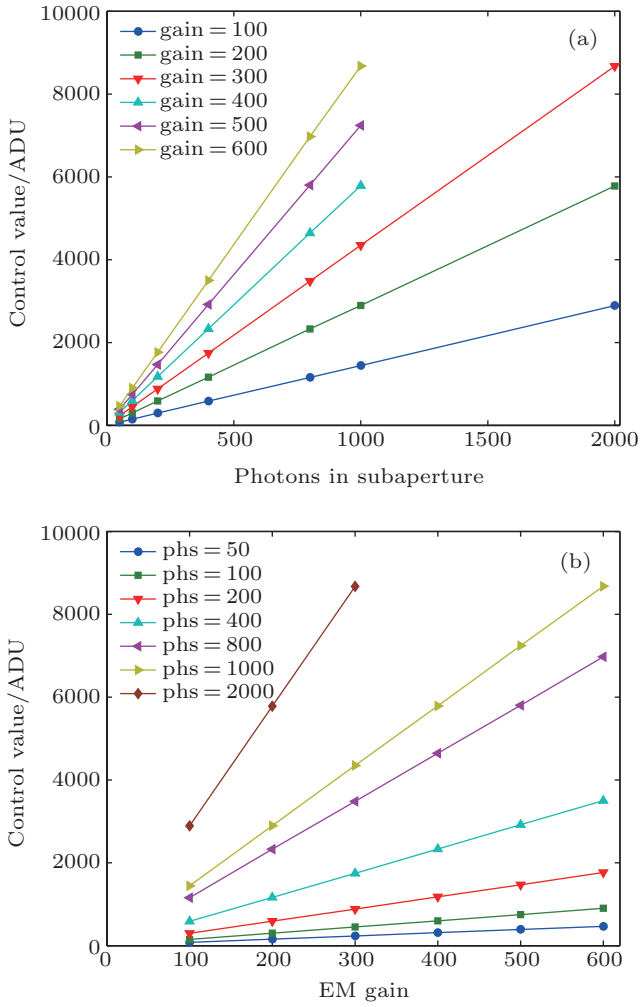


Fig. 5. (color online) Linearity of the average control value with photons collected in (a) sub-apertures and (b) EM gain.

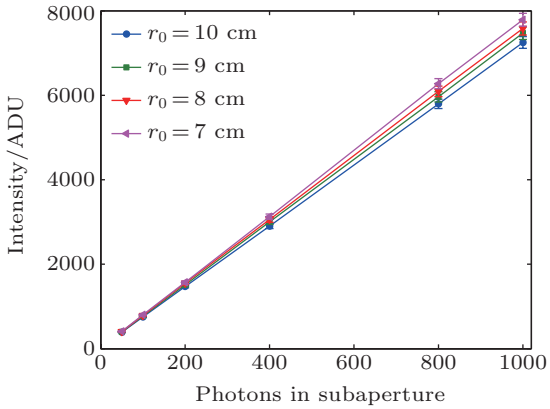


Fig. 6. (color online) Comparison of control values under different strengths of turbulence.

After the characterization, the goal control value was determined. Firstly the maximum signal in a frame must be smaller than the full-well signal of the EMCCD, and the goal control value may be set as $2^{14} \times (0.0145/((0.0295 + 3 \times 0.0022))) \approx 6400$ ADU. Secondly, the goal control value should be examined by the self-protection process, and finally we chose the goal value as 6000 ADU for auto-gain-control.

Considering the missing following situation shown in Fig. 3, we compared the average control values in the situations of different numbers of light spots in a frame. In Fig. 7 the experimental result proved the control value changes a little, which means that under the missing following situation the auto-gain-control still works. The proposed control method was not only stable under the turbulence but also robust under the special case that parts of light spots are missing.

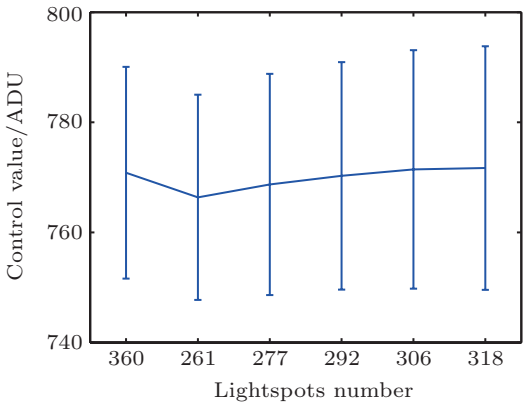
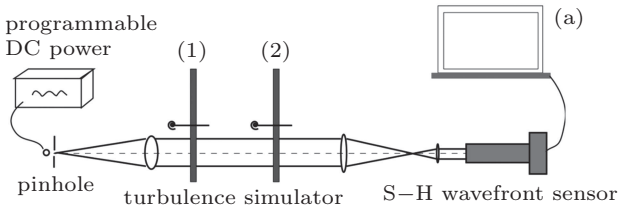


Fig. 7. (color online) Comparisons of control values with different numbers of light spots in a frame.

4. Experimental results and discussion

4.1. Experiment setup

The experimental optical platform was built up and a series of experiments were conducted to verify the proposed auto-gain-control method. The changing brightness of the targets was simulated by a standard light source supplied by a programmable DC power. A group of two turbulence simulators was set in the optical path to generate the atmospheric disturbance.[18,21] The first one was to simulate the scintillation and the second was to generate the turbulent wavefronts. In this experiment a collimated light beam passed through the turbulence simulators and indented into the S–H WFS. The portions of the plates of the second simulator that the light passed through conjugated with the pupil of the S–H WFS. Different sizes of the lit portion would bring different strengths of turbulence. The rotating phase plate could bring changing turbulence into the experiments. The experimental optical system was shown in Fig. 8.



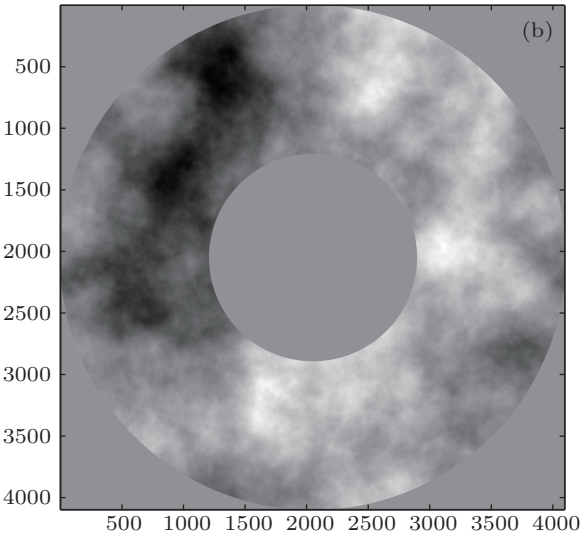


Fig. 8. The experimental optical path for testing the auto-gain-control method. (a) The optical path, (b) the phase plate of the turbulence simulator.

4.2. Results

4.2.1. Linearity test

Firstly, the proposed control value was measured at different brightness and different strengths of turbulence. Figure 9 plots the control value at different numbers of photons collected in a sub-aperture at different strengths of turbulence and in the experiments the sub-aperture diameter was calculated to be $1.25r_0$ and $0.75r_0$. The result was similar to the simulation results. The control value changed a little in different strengths of turbulence and met in a linearity relationship with photons number collected in the sub-apertures. The linear coefficient was also similar to that in the simulations.

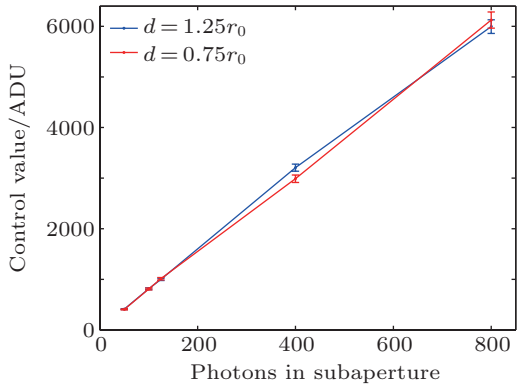


Fig. 9. (color online) Error bar under different strengths of turbulence for different photons collected in a sub-aperture.

4.2.2. Auto-gain-control test

Secondly, we tested the auto-gain-control method in the experiments. We recorded the control value changing with the brightness of the light source without gain control shown in Fig. 10. We could see that the highest brightness is almost twice of the lowest brightness. Figure 11 is the result with auto-gain-control and the goal control value was set

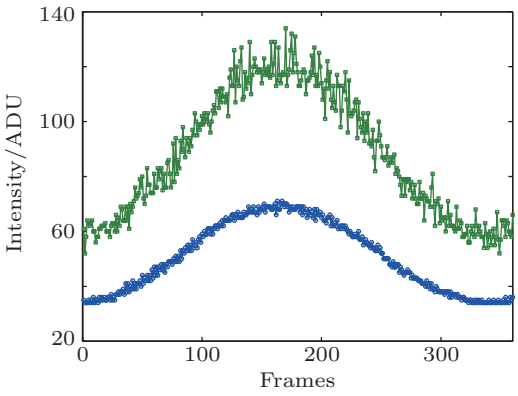


Fig. 10. (color online) The control value and the maximum change without auto-gain-control, measured at $G = 1$.

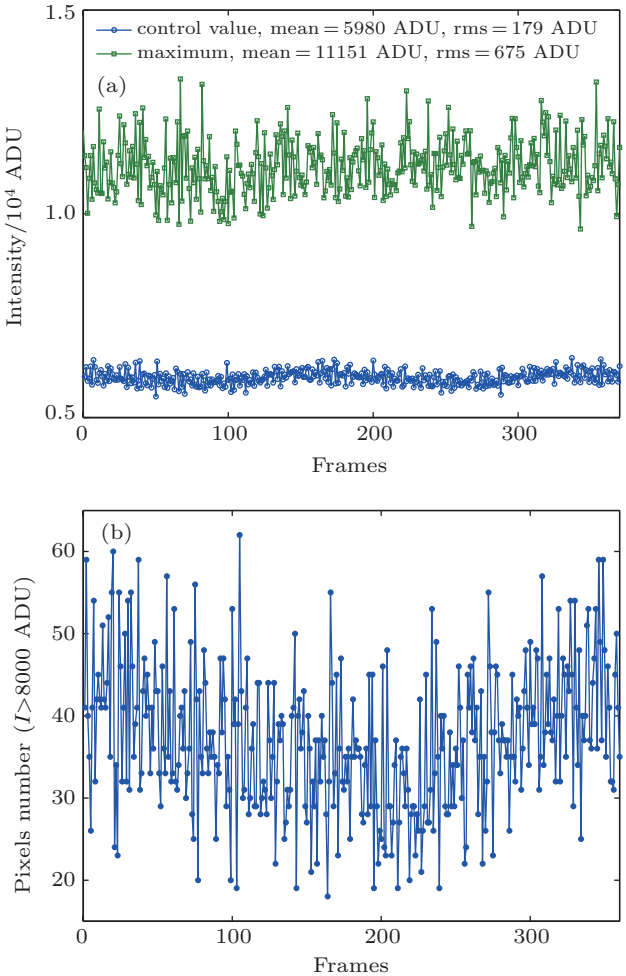


Fig. 11. (color online) Results with auto-gain-control. (a) Comparisons of the control value with the maximum; (b) numbers of pixels with signal larger than 8000 ADU, the numbers are smaller than 100 that did not cause self-protection.

as 6000 ADU as is predetermined. With auto-gain-control the mean of the control values was kept around 6000 ADU, and the RMS results proved the stability and efficiency of the control method from the figures. Numbers of pixels with signal larger than 8000 ADU were recorded during the experiments, shown in Fig. 11(b). During the auto-gain-control test, the numbers were kept less than 70, which would not cause the self-protection of the EMCCD.

The SNR during the test was calculated and plotted in Fig. 12. It is compared with the situations in which fixed gains were set as 100 and 200, respectively. As shown in Fig. 12, when the EM gain was set as 100, the self-protection worked at the frame of number 105, then the gain was reset as 1. So were in the situations that the EM gain was set as 200. In the auto-gain-control test, the SNR was much higher than that without EM gain and the self-protection was avoided. From the definition of the SNR, the SNR in the auto-gain-control test reached the maximum, which is equal to $\sqrt{P/2}$.

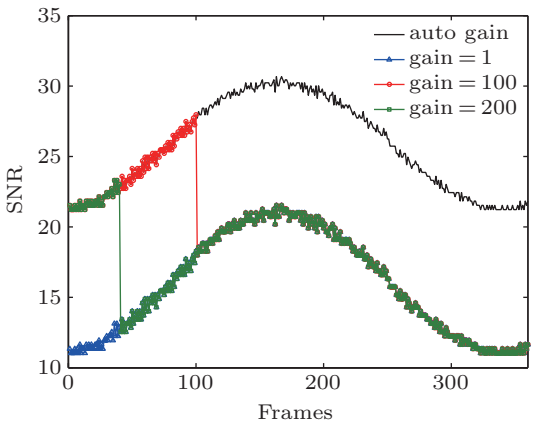


Fig. 12. (color online) The SNR comparisons in the situations of auto-gain-control or fixed gain.

5. Conclusions

An auto-gain-control method suitable for the S–H WFS is proposed. Based on the specialties of the output light-spots arrays of the S–H WFS, a new control value was adopted as the average of the maximum signals of all light spots in a frame. Comparing with the conventional methods, the new method proved its robustness and feasibility. The auto-gain-control method was realized with the EMCCD and verified in experiments. The test results showed that the average control value was stable under turbulence and detecting noise, and was sensitive to the brightness changing of targets. The linearity of the control value with the EM gain and the intensity of targets made it easy to predetermine the goal value, and combined with the self-protection conditions the goal control value was set as 6000 ADU. In the auto-gain-control experiments, the maximum SNR as $\sqrt{P/2}$ working with the EMCCD was achieved for different numbers of photons collected in sub-apertures especially for the dim targets of 6^{mv} to 4^{mv}, and the sensing precision was highly improved. In addition, the self-protection was avoided during the whole process.

References

[1] Martin J B 2014 *Light: Science & Applications* **3** 1
[2] Chen H, Xuan L, Hu L F, Cao Z L and Mu Q Q 2010 *Chinese Journal of Liquid Crystals and Displays* **25** 379
[3] Xuan L, Li D Y and Liu Y G 2015 *Chinese Journal of Liquid Crystals and Displays* **30** 1
[4] Jiang Z, Gong S and Dai Y 2005 *Optics & Laser Technology* **38** 614
[5] Primot J 2003 *Opt. Comm.* **222** 81
[6] Li J, Gong Y, Chen H F and Hu X R 2015 *Opt. Comm.* **336** 127
[7] Lane R G and Tallon M 1992 *Appl. Opt.* **31** 6902
[8] HuangS Y, Ning Y, Xi F J and Jiang Z F 2013 *Opt. Comm.* **288** 7
[9] Nicolle M, Fusco T, Rousset G and Michau V 2004 *Opt. Lett.* **29** 2743
[10] Denvir D J and Conroy E 2002 *Proc. SPIE* **4877** 55
[11] Downing M, Finger G, Baade D, Hubin N, Iwert O and Kolb J 2008 *Proc. SPIE* **7015** 70151R
[12] Feautrier P, Gach J L, Balard P, Guillaume C, Downing M, Stadler E and Magnard Y 2008 *Proc. SPIE* **7021** 70210C
[13] Feautrier P, Gach J L, Balard P, Guillaume C, Downing M, Hubin N, Stadler E and Magnard Y 2010 *Proc. SPIE* **7736** 77360Z
[14] Feautrier P, Gach J L, Balard P, Guillaume C, Downing M, Hubin N, Stadler E and Magnard Y 2011 *Publications of the Astronomical Society of the Pacific* **123** 263
[15] Foppiani I, Baffa C, Biliotti V, Bregoli G, Cosentino G, Giani E, Esposito S and Marano B 2003 *Proc. SPIE* **4839** 312
[16] Qian Y, Zhang W, Liu J, Chen Q and Gu G 2014 *Proc. SPIE* **9273** 92732J
[17] Fowler K R 2004 *Proc. IEEE Transactions on Instrumentation and Measurement* **53** 1057
[18] Dayton D, Pierson B and Spielbusch B 1992 *Opt. Lett.* **17** 1737
[19] SamPat N, Venkataraman S, Yeh T and Kremens R 1999 *Proc. SPIE* **3650** 100
[20] Denvir D J and Conroy E 2003 *Proc. SPIE* **4796** 164
[21] Mantravadi S V, Rhoadarmer T A and Glas R S 2004 *Proc. SPIE* **5553** 290